Oil-water flow regimes in 4-mm borosilicate glass and fluorinated ethylene propylene channels: Effects of wall wettability

G.A. Riley[a], K.K Bultongez[a], M.M Derby[a,*]

[a]Department of Mechanical and Nuclear Engineering, Kansas State University, Manhattan, KS 66506 USA

[*]corresponding author: derbym@ksu.edu, 1701B Platt St., Manhattan, KS 66506, USA,

Tel: 785-532-2606, Fax: 785-532-7057

Abstract:

Formation water, found in oil deposits, is highly corrosive. By utilizing flow phenomena and surface tension forces in smaller channels (e.g., Eötvös number less than one), these fluids can be separated, thus altering corrosion and the pressure required for transport. This research investigates the effects of wall wettability on oil-water flow regimes and pressure drops. Oil-water flows were studied in 3.5-mm hydrophilic borosilicate glass and 4.0-mm hydrophobic fluorinated ethylene propylene (FEP) channels using Parol 100 mineral oil (i.e., density of 840 kg/m^3 and viscosity of 0.0208 Pa·s) and tap water (i.e., 997 kg/m^3 and a viscosity of 0.001 Pa·s). For these oil-water combinations, glass was water wetting (i.e., contact angle of 67^o for a water droplet submerged in oil on glass) and FEP was water repelling (i.e., contact angle of 93^o for a water droplet submerged in oil on FEP) under static conditions. Flow regimes and pressure drops were recorded for a range of oil superficial velocities [i.e., 0.31–3.7 m/s (glass) and 0.23–2.7 m/s (FEP)] and water superficial velocities [i.e., 0.080m/s–5.5 m/s (glass) and 0.060–5.5 m/s (FEP)]. Stratified, intermittent, annular, and dispersed flow regimes were observed in both tubes. Additional inverted and dual flow regimes were observed in the hydrophobic FEP; oil wetted the wall in inverted flows, and flow regimes occurred inside of another flow regime in dual flows (e.g.,

inverted-annular intermittent). The modified Weber number indicated whether the walls were wetted by oil, mixed oil and water, or water. Pressure drops were found to be correlated to the flow regime with increased pressure drops observed when oil fully or partially wetted the wall.

Keywords: multiphase flow; fluid dynamics; oil-water interface; capillarity

GRAPHICAL ABSTRACT

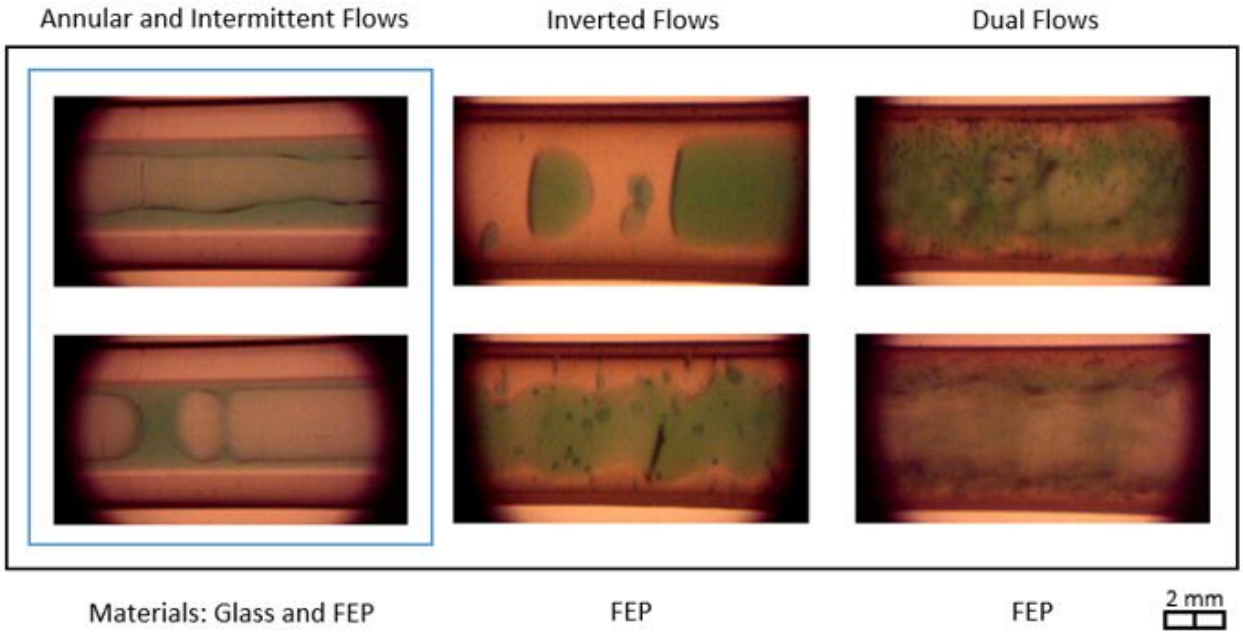

The water has been dyed green for contrast and the oil appears clear.

HIGHLIGHTS

- Investigated oil-water flows in hydrophilic and hydrophobic 4-mm channels
- Stratified, intermittent, annular, and dispersed flow regimes in both channels
- Inverted (i.e., oil wetting) flow regimes observed in the hydrophobic channel
- Pressure drops depended on flow regimes, tube material, and wetting fluid

1. INTRODUCTION

Oil-water flows are of great interest to industry, including water-lubricated transport (i.e., annular flow) of heavy crude [1], reducing corrosion due to water wetting the pipe wall [2], and separating oil-water mixtures [3]. However, there are competing priorities. Water wetting, or

hydrophilic/oleophobic walls, are desirable for reducing pressure drops [4], but the presence of water at the pipe wall accelerates corrosion [2], and thus hydrophobic/oleophilic walls are desirable for reducing corrosion. Oil-water pressure drops and corrosion rates rely heavily on the resulting oil-water flow regime. Different flow regimes appear in mini-channels (e.g., 200 μm < D_h < 3 mm [5]) compared to conventional-size channels (e.g., D_h > 3 mm [5]) due to the relative importance of surface tension to gravity forces in smaller channels [6]. Flow regime maps developed for air-water flows [7, 8], and liquid-vapor flows during condensation [9, 10] and boiling [11, 12] do not directly apply to oil-water flows due to comparable oil-water densities and large oil-water viscosity ratios [6, 13]. Additionally, wall wettability—i.e., whether oil or water is in contact with the wall—affects flow regimes and is therefore an important research topic for oil transport and reducing corrosion.

For glass or stainless steel mini-channels, common oil-water flow regimes observed in mini-channels include intermittent (e.g., slug/plug flow), annular (e.g., water at the wall and oil at the core), and dispersed flows (e.g., oil-in-water or water-in-oil) [3, 4, 6, 14, 15]. As pipe diameters increase, gravitational effects are more apparent in forming stratified flows (e.g., water in contact with the bottom of the tube and oil in contact with the upper tube wall) [16-18]. There is an interest in exploring a range of materials to alter the wall wetting fluid. da Silva [19] investigated contact angles of PVC; glass; and stainless, enameled, and galvanized steels for water-lubricated pipeline transport. Glass surfaces had less oil wetting than steel. Oxidizing the materials created hydrophilic rather than oleophilic walls and they observed that both the surface properties and oil composition affected contact angles. Arney et al. [20] studied oil-water flows in 2.43- to 2.65-cm pipes coated with portland cement to make the walls oleophobic and hydrophilic; the cement coating reduced fouling during lengthy tests.

A combination of wall materials, oil composition, and flow conditions may affect whether oil or water wets the tube wall [2, 4, 18, 21-24]. For certain combinations, inverted annular flows occur in which oil is fully or partially in contact with the tube wall. The core flow can be all water or a mixture of oil and water. This inverted annular flow condition, combined with oil-selective membranes, may be used to separate oil from formation water after the wellhead. Andreini et al. [4] observed dispersed, annular, and intermittent flows in 3.1-mm and 6-mm mini-channels. However, at low velocities (i.e., water superficial velocities divided by oil superficial velocities < 0.2–0.3) in the 6-mm tube, they observed inverted annular flows in which oil wetted the wall and oil flowed in the core.

Oil wetting and inverted flows have been observed in conventional-size tubes, particularly at low superficial velocities. Cai et al. [2] studied wetting phenomena in a 0.1-m-diameter, 14-m-long stainless steel pipe. Due to the large diameter of the pipe, wetting was primarily a function of flow regime, with oil wetting at low cuts (i.e., <10%), water wetting at higher water cuts (i.e., >15%) and low total superficial velocities (i.e., <1 m/s), and intermittent wetting (i.e., alternating water/oil wetting) at conditions in between. Ismail et al. [21] studied pressure drops and flow regimes of Malaysian light waxy crude and synthetic formation water in a 5.08-cm tube. Oil was in contact with the acrylic tube wall at low flow rates and over a range of water cuts. The authors noted that the multi-parameter composition of the Malaysian light waxy crude and oil-wetting acrylic surface likely contributed to this behavior. Wang et al. [22] studied crude oil-water flow regimes and pressure drops in a 25.4-mm, stainless steel tube. The study observed flow patterns that were combinations of water-in-oil emulsions with stratified, intermittent, annular, and dispersed flow regimes. In the oil-dominated regimes found (e.g., at water fractions <50%), the authors observed some water-in-oil dispersed flows in which oil partially wetted the tube wall. The

review by Xu [23] highlighted the phase inversion point, a sudden switch between oil-in-water dispersions to water-in-oil dispersions and vice versa and noted in linkage between wall-wetting fluid and corrosion. These phase inversions can also affect pressure drops [25].

Capillary, or surface tension forces, are of primary interest as diameter decreases. Tsaoulidis et al. [26] investigated ionic fluid-water flows in glass, FEP and Tefzel with tube diameters of 200 μm, 220 μm, 270 μm respectively. Wettability was an important factor that affected flow regimes in glass (i.e., contact angle of water-in-air of 55^{o}) and Teflon (i.e., contact angles of water-in-air of 102^{o}) tubes. The authors observed that flows in the glass tube were highly affected by the fluid that first wetted the channel. In all flow regimes, water was the continuous phase and in full contact with the glass tube walls. Plug and intermittent flows were primarily observed in glass tubes, while annular flow was encountered in the Teflon tubes, with water flowing in the core, plug flow and drop flow, with water being the encapsulated liquid. Brauner et al. elaborated on this phenomena occurring in the hydrophobic tubes and named it inverted annular flow [27]. At the lower diameter range of mini-channels, oil-water flow regimes depend on whether oil or water first fills the channel, and stratified flows were not observed due to the increased importance of surface tension over gravity [28, 29]. At even smaller size micro-scales, capillary forces governed imbibition in fabricated, pore-scale geometries [30, 31].

Few studies have examined the impacts of wall materials and flow conditions on flow regimes and wall wetting for mini-channel oil-water flows. The research objectives of this work are to investigate oil-water flow regimes in 3.5- and 4.0-mm glass and fluorinated ethylene propylene (FEP) tubes. For these oil-water combinations, glass is water wetting and FEP is oil wetting under static conditions. Additionally, both channels have an Eötvös number below one, selected because surface tension forces between the fluids will dominate over gravitaional forces;

the *Eö* numbers in the glass and FEP are 0.4 and 0.6, respectively. The focus of this research is to determine fundamental flow regimes in glass and FEP tubes in order to design systems to separate oil and water after the wellhead; future work will need to consider higher temperatures and pressures.

2. MATERIALS AND METHODS

2.1 Tube Materials and Fluid Properties

Oil-water flows were studied in 3.5-mm borosilicate glass and 4.0-mm fluorinated ethylene propylene (FEP) tubes. The borosilicate glass is hydrophilic (i.e., water contact angle of 18°), whereas the FEP is hydrophobic (i.e., contact angle of 91°) under static conditions between water and air; goniometer images with water and air are shown in Figure 1a. Both materials are oleophilic with contacts angles of 36° and 44° on glass and FEP respectively as shown in Figure 1b. Experiments were conducted using tap water (e.g., ρ=997 kg/m^3, μ=0.001 Pa·s)—dyed green for visualization—and Parol 100^{TM} mineral oil (e.g., ρ=840 kg/m^3, μ=0.0208 Pa·s). Campus tap water properties were reported by Schmitz [32]. The electrical conductivity was 0.2 dS/m, pH was 8.7, and the concentrations of the following chemicals were reported: S, K, Na, Mg, Ca, Chloride, NO3-N and NH4-N were 19, 8, 31, 15, 14, 58, 0, and 1 mg/L respectively. Interfacial tensions between Parol 100 and tap water were 38.8 mN/m and were measured using the pendant drop method conducted by Augustine Scientific [33]. The contact angle of water submerged in oil was also measured by Augustine Scientific, resulting in water-oil contact angles of 67^o on glass and 93^o on FEP, as shown in Figure 2a and 2b, respectively. For this oil-water combination, glass is hydrophilic and FEP is hydrophobic.

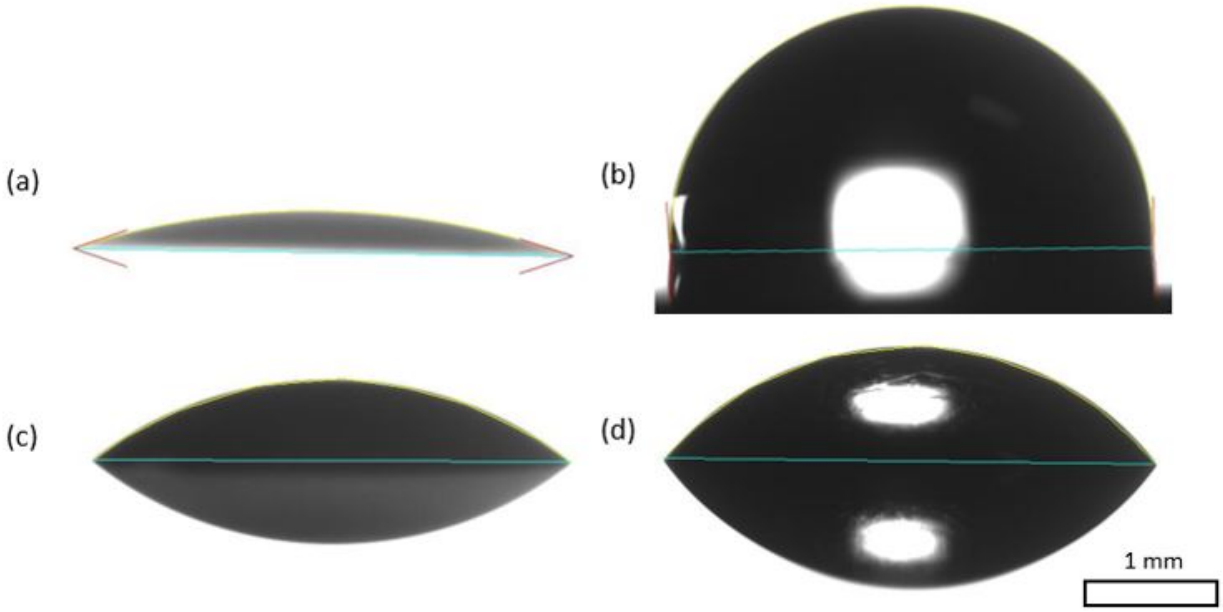

Figure 1: Contact angles of water surrounded by air for (a) water on glass, (b) water on FEP, (c) oil on glass, and (d) oil on FEP.

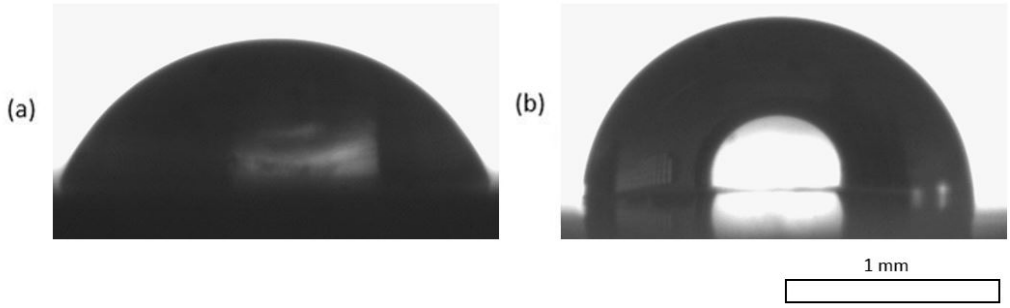

Figure 2: Contact angles of water submerged in oil for (a) glass and (b) FEP

2.2 Experimental Apparatus and Test Section

The experimental apparatus, shown in Figure 3, was an adiabatic, closed-loop system. Oil and water were stored in a 30-galUS tank and were transported independently by two pumps (GC-M25.PS5S.E, Micropump) controlled via variable frequency drives. Water was sourced from the bottom of the tank and oil from the top; the measured densities confirmed that the two fluids were

not mixed. Each fluid passed through its respective Coriolis flowmeter (CMFS015M, Micro Motion) where the fluid's mass flow rate, density, and temperature were measured before mixing in a y-junction. The oil-water mixture then flowed through a 680-mm-long channel, which allowed the flow to fully develop before entering the test section shown in Figure 4. The pressure differential across the test section was measured via a 50-psi pressure transducer (Setra) with ±0.25% full scale accuracy. To measure the pressure drop, holes were drilled into the FEP channel at the T-junctions (Figure 4). For the glass channel, custom-made inserts were fit inside the T-junction and allowed for the pressure measurements to be recorded. Both test section lengths were 387 mm. The two-phase flow entered the tank and the oil-water flow was separated using gravity. Flow regimes were visualized through the channel wall of the test section using a high-speed camera (Fastec IL5) with a microscope (Leica S6 D).

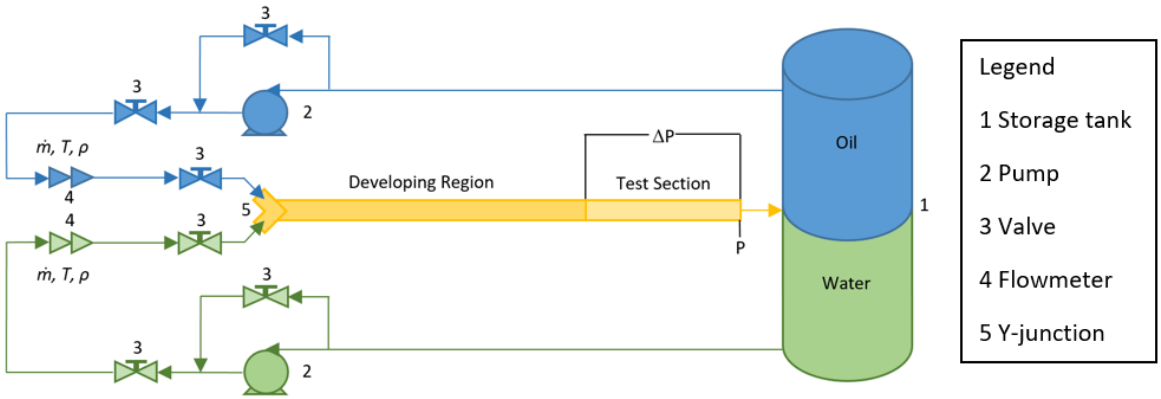

Figure 3: Experimental apparatus.

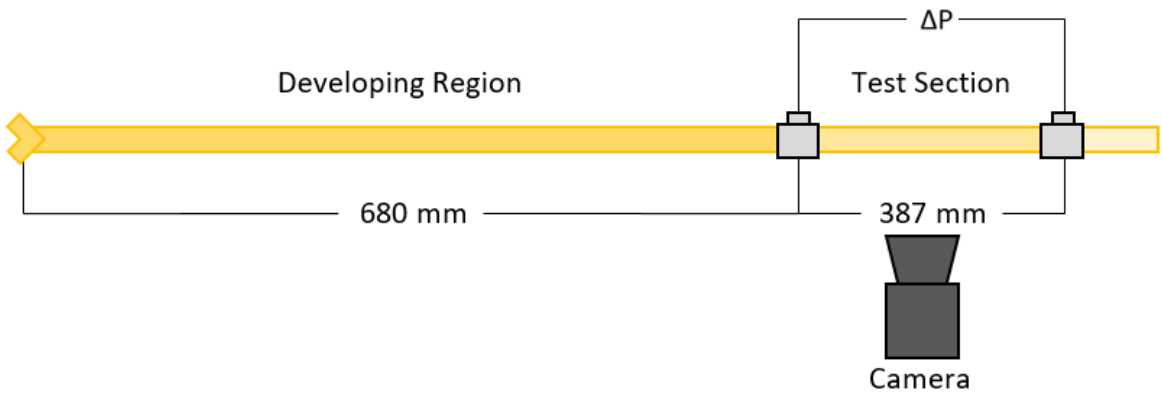

Figure 4: Test section for pressure drop measurement and flow visualization.

2.3 Experimental Procedures

The desired flow conditions were reached by independently controlling oil and water mass flow rates, and data are presented in terms of the superficial velocities, j, and the water input ratio, ε. The superficial velocity is the mass flow rate of the fluid, $\dot{m}$, divided by its density, ρ, and the total cross-sectional area of the channel, A,

$$j_w = \frac{\dot{m}_w}{\rho_w A} \quad (1) \qquad j_o = \frac{\dot{m}_o}{\rho_o A} \quad (2)$$

where subscripts w and o correspond to water and oil, respectively. The water input ratio is the water superficial velocity divided by the combined superficial velocity of both the oil and water,

$$\varepsilon = \frac{j_w}{j_o + j_w} = \frac{\dot{m}_w}{\frac{\rho_W \dot{m}_o}{\rho_o} + \dot{m}_w} \quad (3)$$

and, therefore, the water-oil density ratio and relative mass flow rates impact the water input ratio.

For two-phase experiments, the experimental data were collected using the following procedure:

1. An oil mass flow rate was selected and water input ratios were specified in increments of 0.1.

2. The water mass flow rates required for the water input ratio range were calculated using equation (3).

3. Water was introduced into the system and set approximately to the lowest flow rate being tested.

4. Oil was introduced to the system and both oil and water flow rates were adjusted until desired values were reached with minimal fluctuations.

5. After steady state occurred, pressure, temperature, mass flow rate, and density measurements were recorded. Still images and video of flow regime were taken.

6. Water flow rate was increased to achieve next lowest water input ratio.

7. Steps 5 and 6 were repeated until data for all water input ratios has been collected.

8. Return to Step 1 with new oil mass flow rate and repeat the process.

Data were collected and analyzed for a given oil flow rate at all water flow rates achievable in the experimental apparatus. In addition to the previously stated procedure, two to three data points per oil flow rate were repeated for verification of flow regime and pressure drop.

3. RESULTS AND DISCUSSION

3.1 Observed Flow Regimes in the Glass Tube

Flow regimes observed in hydrophilic millimeter tubes, such as borosilicate glass, can be classified as stratified, intermittent, annular, and dispersed [3, 4, 15] (Figure 5). In stratified flows (Figure 5a), the oil and water are separated by gravity and the less dense fluid flows above the denser fluid. Stratified flow is an example of mixed wetting (i.e., wall wetted by both oil and water) and occupied a small fraction of flow conditions due to the low Eötvös number of these channels. Intermittent flows are similar to annular flows in which a water annulus surrounds an oil core and is periodically separated by periods of water flow only (Figure 5b). For annular flows in these

channels, water completely wetted the surface and an oil core flows through the water annulus (Figure 5c). In dispersed flows, the oil and water are mixed such that no clear boundary between the two fluids exists (Figure 5d). These flow regimes can be further classified based on the presence of waves at the oil-water interface and fluid wetting the tube wall; water wetted the wall in annular, intermittent, and dispersed flows.

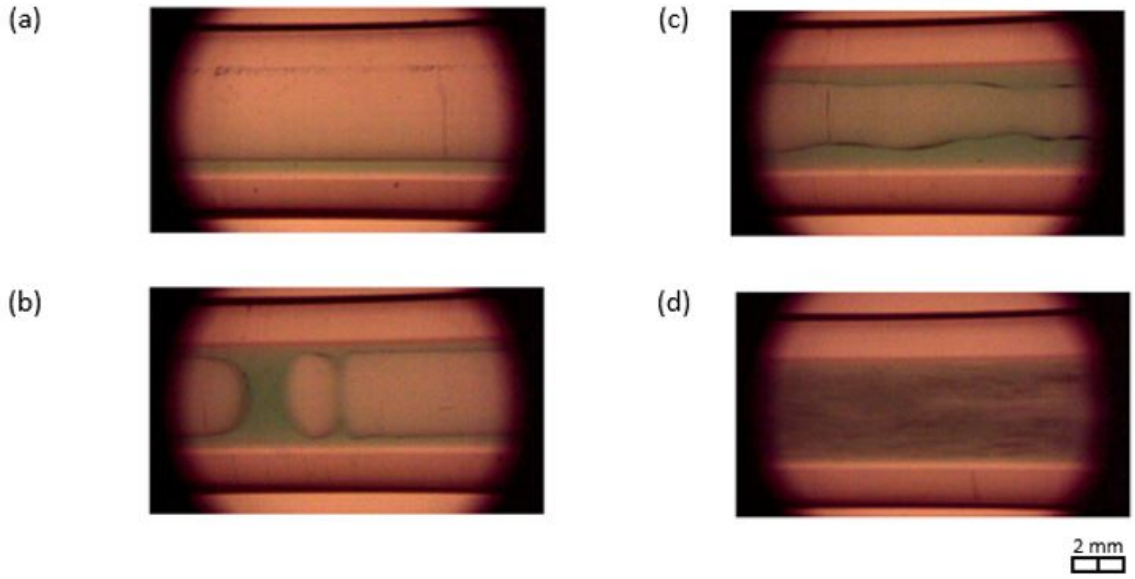

Figure 5: Hydrophilic flow regimes—(a) stratified, (b) intermittent, (c) annular, and (d) dispersed.

3.2 Observed Flow Regimes in the FEP Tube

Stratified, intermittent, annual, and dispersed flows were observed in the 4.0-mm FEP tube (Figure 6a, j, k, l) in addition to inverted or dual flow regimes [2, 4, 21, 22]. An additional eight distinct flow regimes were identified in the FEP mini-channel that are described as being either inverted (e.g., with oil wetting the wall and a water core flowing through it) [25, 34], flow with a rivulet [35], or a dual flow in which a flow regime occurring inside of another flow regime (e.g.,

206 in an inverted-annular intermittent flow oil is wetting the wall and forms and annulus through
207 which a water core flows with an intermittent oil core inside the water core).

208 Due to the hydrophobicity of FEP, oil wets the tube wall in inverted flows. In Figure 6, all
209 twelve flow regimes observed in the FEP are shown. Inverted flows are notated as “inverted-flow”,
210 dual flows are listed as “inner flow-outer flow”, and flows with a rivulet are described as “flow
211 with rivulet”. In inverted-intermittent (Figure 6b), inverted-annular flows (Figure 6c), and
212 inverted-dispersed (Figure 6d), oil wets the tube wall and an intermittent or continuous water core
213 flow is formed. Inverted-intermittent intermittent flow consists of an oil-wetting annulus through
214 which a core of water will periodically flow through with an oil core intermittently flowing through
215 the water core (Figure 6e). Inverted-annular annular and inverted-annular intermittent flows occur
216 when the water core inside of the wetting oil annulus has either a continuous or intermittent core
217 of oil flowing through it (Figure 6f and g). Annular with oil rivulet and intermittent with oil rivulet
218 are similar to common annular and intermittent flow regimes but have a rivulet of oil that flows
219 along the top of the channel, wetting a portion of the wall (Figure 6h-i).

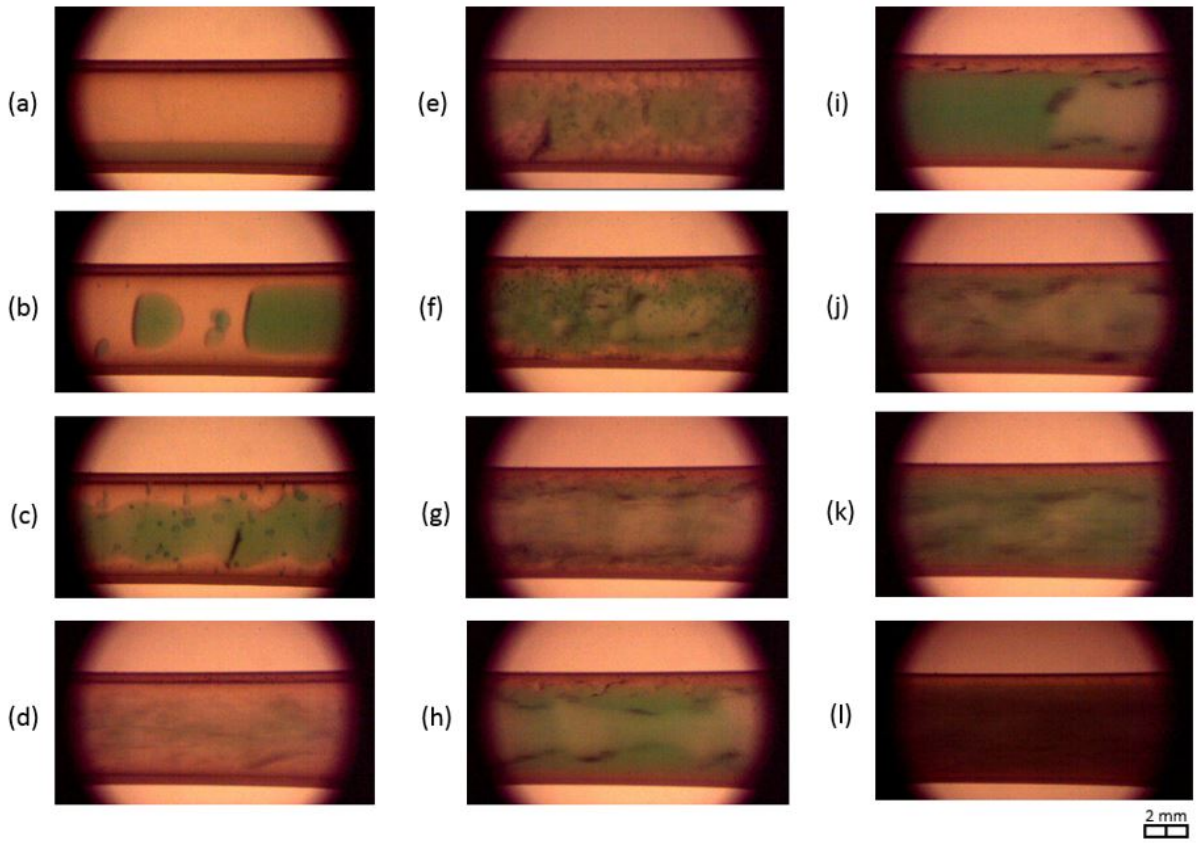

Figure 6: Hydrophobic flow regimes—(a) stratified, (b) inverted-intermittent, (c) inverted-annular, (d) inverted-dispersed, (e) inverted-intermittent intermittent, (f) inverted-annular intermittent, (g) inverted-annular annular, (h) annular with oil rivulet, (i) intermittent with oil rivulet, (j) annular, (k) intermittent, and (l) dispersed.

3.3 Flow Regime Maps

Flow regimes are mapped for the glass (Figure 7) and FEP (Figure 8) tubes. In both tube materials, stratified flows occurred when the total superficial velocity was low (i.e., j_o<1.28 m/s, j_w <0.20 m/s). In the glass mini-channel, annular flow was the dominant flow regime when the oil flow rate was greater than the water flow rate (i.e., 0.31 m/s<j_o<3.7 m/s, 0.26 m/s<j_w<2.5 m/s); conversely, intermittent flows dominated when the water flow rate was higher than that of the oil (i.e., 0.31 m/s<j_o<3.7 m/s, 0.48 m/s<j_w<3.7 m/s). For the largest water flow rates (i.e., 3.7 m/s<j_w),

dispersed flows were observed. These flow regimes are commensurate with those observed in previous mini-channel oil-water flow research [3, 28, 36]; macro-scale channels exhibit stronger gravity impacts and stratified flow is typically the dominant flow regime [6, 37], whereas surface tension is a key driver in micro-channel flow regimes [30, 31].

For the FEP mini-channel, as the superficial velocity increased (i.e., j_{tot} > 0.38 m/s), the flow regimes become inverted, oil wetting (Figure 8). As the oil flow rate progressed from lowest (i.e., j_o=0.23 m/s) to highest (i.e., j_o=2.7 m/s) in the inverted region, the flow regimes trended from inverted-annular to inverted-intermittent to inverted-dispersed. Further increasing the water flow rate (i.e., 0.33 m/s<j_w<1.2 m/s) lead to the dual flows, which, with an increasing oil flow rate, tend from inverted-annular intermittent to inverted-annular annular. Inverted-intermittent intermittent flows occurred in the region between inverted-intermittent and inverted-annular intermittent flows. After the water flow rate was further increased (i.e., 1.4 m/s<j_w<2.1 m/s), the flow regimes developed oil rivulets in conjunction with either an intermittent flow, mixed wetting, for lower oil flow rates (i.e., j_o=0.91 m/s), or an annular flow, for higher oil flow rates (i.e., 1.4 m/s<j_o<2.7 m/s). The oil rivulets disappeared as the water flow rate was further increased (i.e., 1.8 m/s<j_w<3.4 m/s) and the flow regimes were either intermittent or annular, water wetting, depending on the oil flow rate. As with the glass, for the highest total superficial velocities, the flow regime was dispersed.

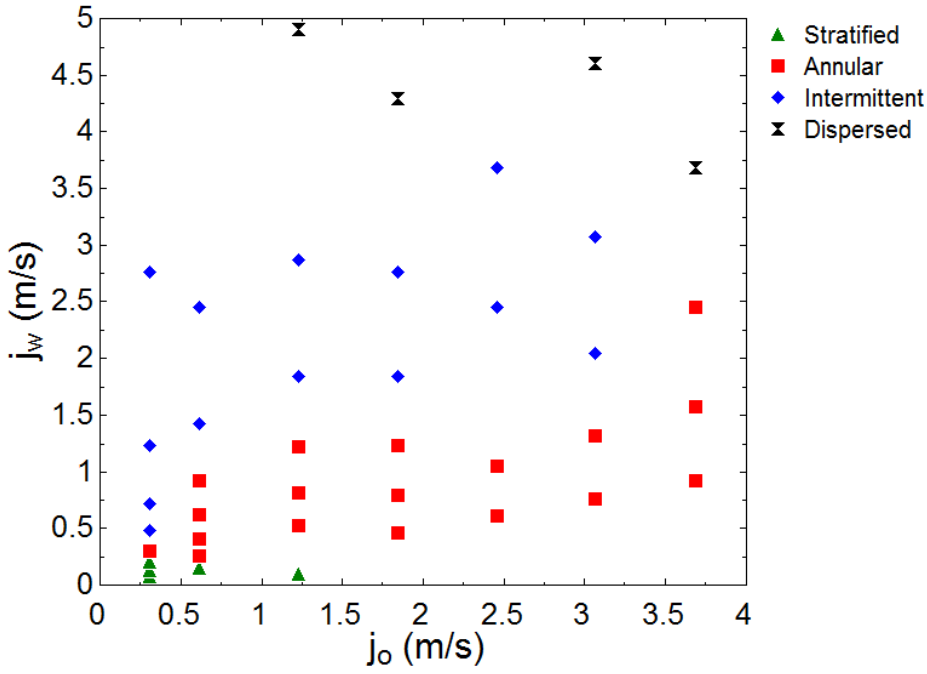

Figure 7: Flow regimes in the glass tube—mixed oil-water wetting in stratified flows and water wall wetting in annular, intermittent, and dispersed flows.

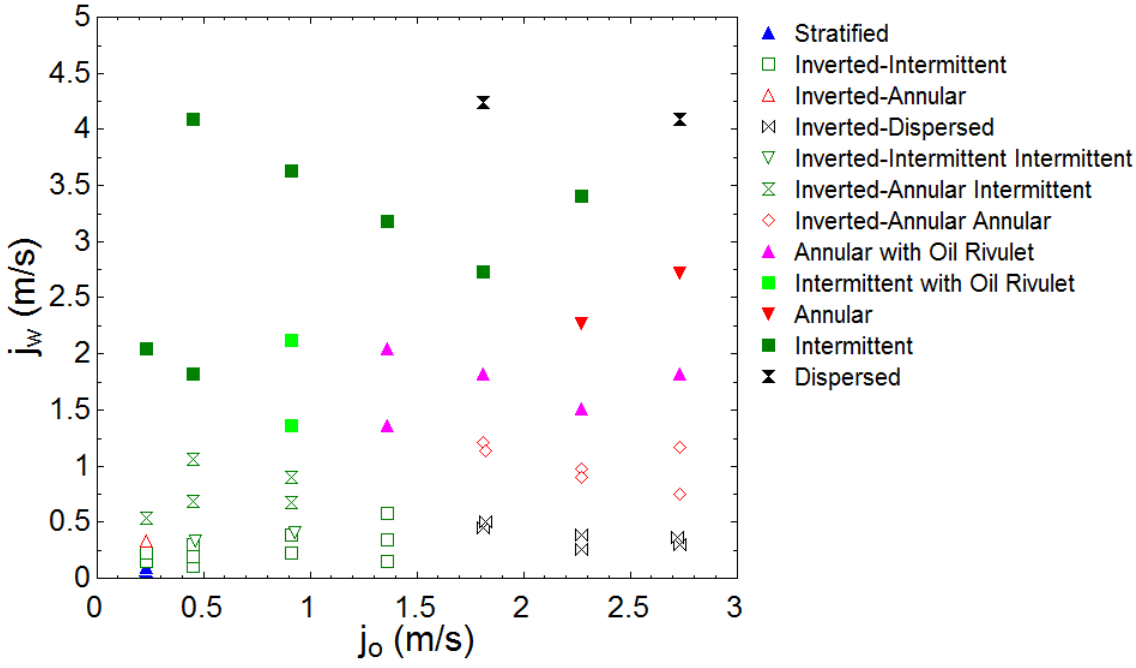

Figure 8: Flow regimes in the FEP tube.

To better understand the presence of oil wetted flow regimes (e.g., inverted-intermittent), an analysis using the modified Weber number (*We**) was conducted. *We** is the ratio between inertial and surface tension forces between fluids, which Kim and Mudawar [38, 39] used to determine transition regions between flow regimes in two phase condensers. For the purpose of adapting these equations to liquid-liquid flows, oil was approximated as the liquid, water as the gas, and the quality as j_w/j_{tot},

$$We^* = 2.45\frac{Re_w^{0.64}}{Su_w^{0.3}(1+1.09X_{tt}^{0.039})^{0.4}} \text{ for } Re_o \leq 1250 \quad (4)$$

$$We^* = 0.85\frac{Re_w^{0.79}X_{tt}^{0.157}}{Su_w^{0.3}(1+1.09X_{tt}^{0.039})^{0.4}}\left[\left(\frac{\mu_w}{\mu_o}\right)^2\left(\frac{\nu_w}{\nu_o}\right)\right]^{0.084} \text{ for } Re_o > 1250 \quad (5)$$

$$Su_w = \frac{\rho_w \sigma D}{\mu_w^2} \quad (6)$$

$$X_{tt} = \left(\frac{\mu_o}{\mu_w}\right)^{0.1}\left(\frac{1-j_w/j_{tot}}{j_w/j_{tot}}\right)^{0.9}\left(\frac{\nu_o}{\nu_w}\right)^{0.5} \quad (7)$$

Kim and Mudawar determined that when *We** was greater than $7X_{tt}^{0.2}$, the flow regime would be annular, but when *We** was less than $7X_{tt}^{0.2}$, slug flow would be present. In Figure 9, $7X_{tt}^{0.2}$ is shown verses *We** in the FEP channel. Flow regimes in which oil was the primary wetting fluid (e.g., stratified, inverted-annular) occur where *We** was greater than $7X_{tt}^{0.2}$ and *We** was less than $7X_{tt}$ when water was the primary wetting fluid (e.g. annular with oil rivulet, intermittent).

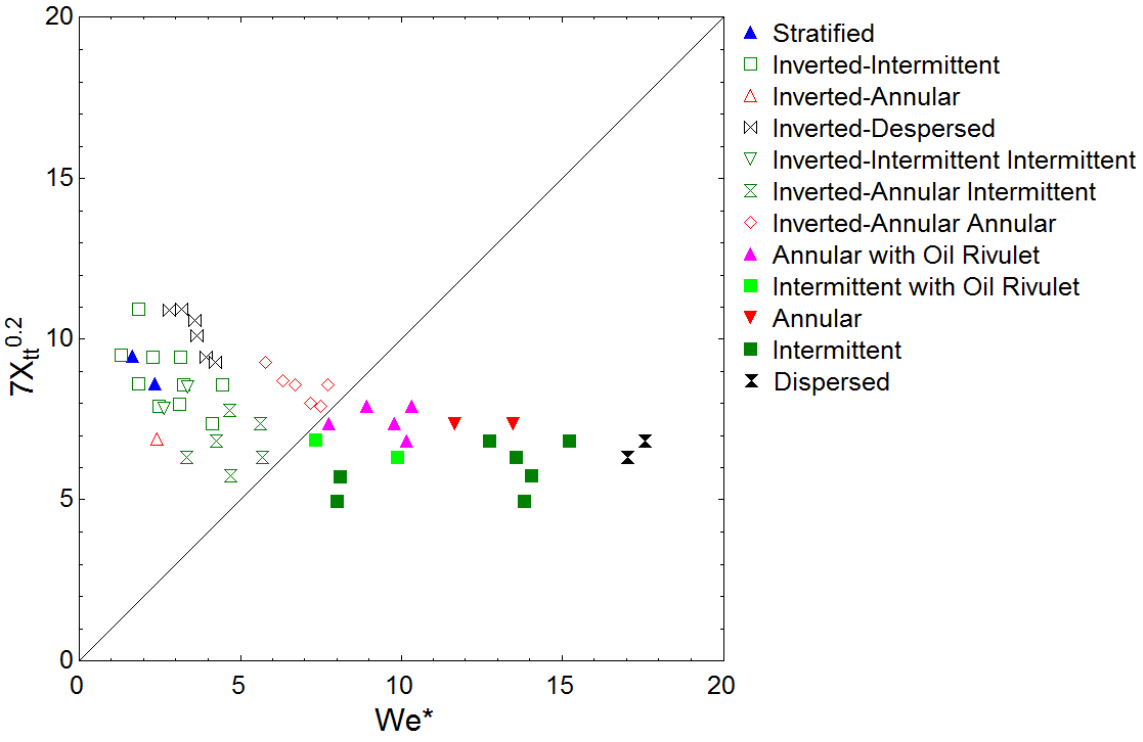

Figure 9: Modified Weber number analysis regarding wall wetting in the FEP tube.

3.4 Pressure Drops

In borosilicate glass, measured pressure drops were primarily a function of the water input ratio and oil flow rate. In general, pressure drop followed a parabolic trend as the water input ratio increased for a particular oil flow rate; this corresponded to a higher total superficial velocity. Flow regimes affected pressure drops for the lowest superficial velocities where the stratified flow occurs. In stratified flow, both oil and water are wetting the surface.

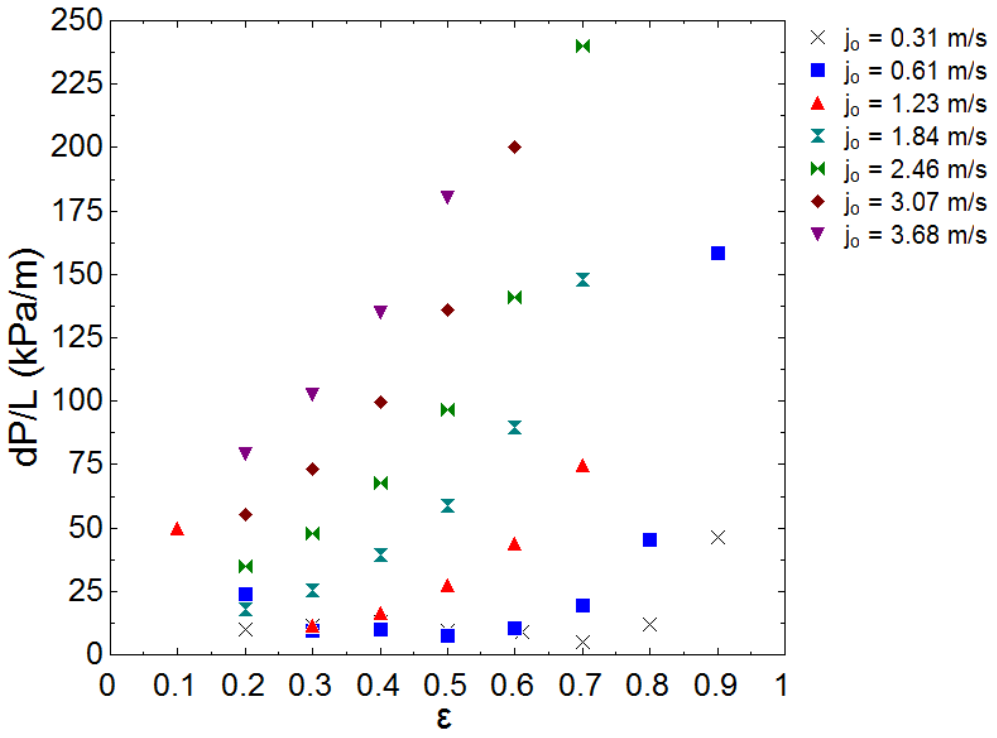

Figure 10: Pressure drops in the borosilicate glass tube.

In the FEP mini-channel, the effects of flow regime on the pressure drop were much more significant. A comparison between the pressure drops and flow regimes in glass and FEP is shown in Figure 12 for an oil superficial velocity of 1.8 m/s. The pressure drop is initial as high as 250 kPa/m when the flow is inverted and oil wets the wall. As the flow regime transitions from inverted to dual flow, a significant pressure drop occurs as the water annulus is acting as a lubricant for the oil core. This flow regime change typically occurs when ε is between 0.2 and 0.4. A smaller pressure decrease then occurs with a dual flow (e.g., inverted-annular intermittent) transitions to a flow with rivulet (e.g., intermittent with oil rivulet). At this point, the pressure drop changes in a way consistent with what has been observed in hydrophilic materials such as borosilicate glass (i.e., increasing with increasing water input ratio).

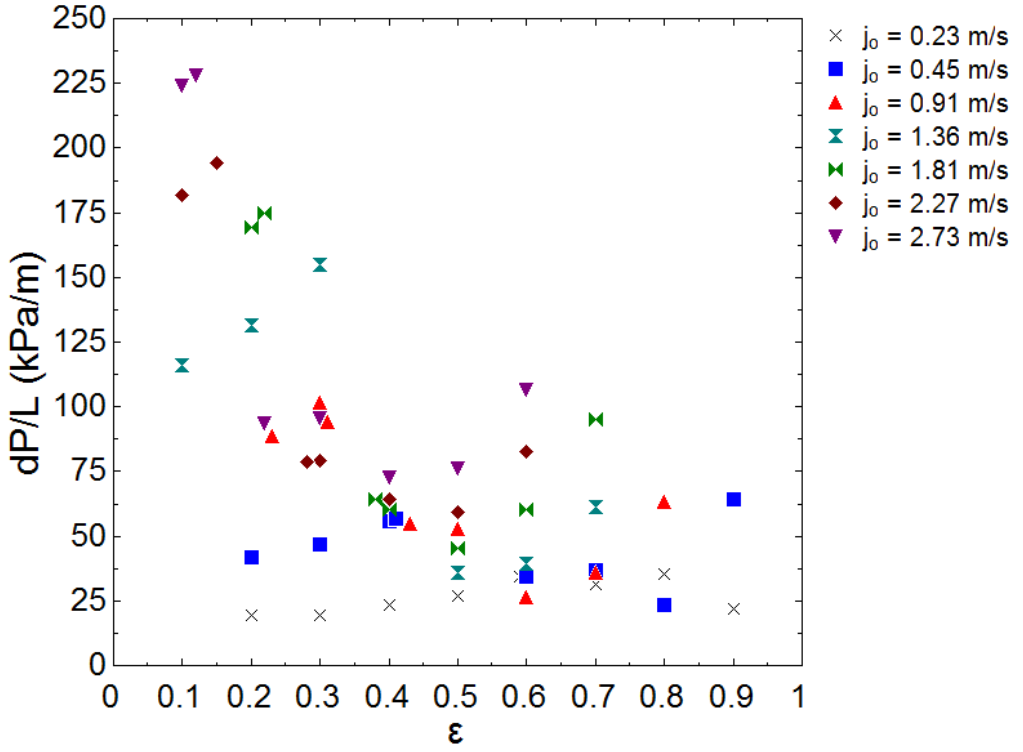

289

290 *Figure 11: Pressure drops in FEP are a strong function of flow regime.*

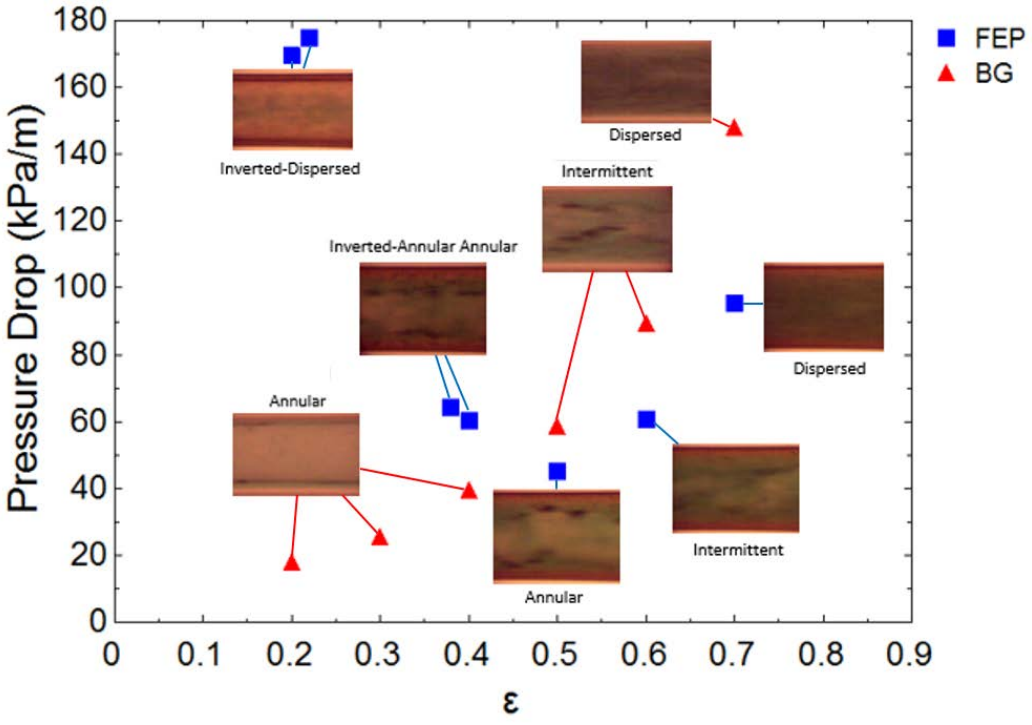

291

292 *Figure 12: Pressure drops and flow regimes at j_o = 1.8 m/s for both the glass and FEP tubes.*

4. CONCLUSIONS

Flow regimes and pressure drops were observed and measured in hydrophilic glass and hydrophobic FEP channels with Eötvös numbers less than one. Flow regimes and pressure drops varied over a range of oil and water flow rates. The conclusions drawn from the study are as follows:

- Stratified, annular, intermittent, and dispersed flow were observed in both channels.
- Additional flow regimes, including inverted-intermittent, inverted-annular, inverted-dispersed, inverted-intermittent intermittent, inverted-annular intermittent, inverted-annular annular, annular with oil rivulet, and intermittent with oil rivulet, were observed in the hydrophobic channel.
- Oil and water wetting flow regimes in FEP were found to relate to the relative values of $7X_{tt}^{0.2}$ and We^* for each set of flow rates.
- Pressure drops in both channels were dependent on the flow regime and wetting fluid and especially apparent in the FEP.

The ideal oil-water flow regime depends on the desired transport or separation requirements. While water-wetting annular flows offered the lowest pressure drop, the corrosive nature of salt water means that an oil-wetting flow may be preferable during transportation in conditions where corrosion is very costly. Of the oil-wetting flow regimes, the inverted-annular intermittent and inverted-annular annular flows offer the lowest pressure drop. In inverted-annular flow regimes, oil wets the fluid wall and may be removed from the water using oil-selective membranes. Due to material limitations, this study does not account for the effects of extreme temperature and pressure on fluid properties and flow regimes, as encountered in reservoirs. It is recommended that the effects of these parameters should be examined in future studies.

NOMENCLATURE

A	Area (m^2)
D	Diameter (m)
$Eö$	Eötvös number (-)
Re	Reynolds number (-)
Su	Suratman number (-)
We^*	Modified Weber number (-)
X	Martinelli parameter (-)
j	Superficial velocity (m/s)
$\dot{m}$	Mass flow rate (kg/s)
ε	Water input ratio
μ	Dynamic viscosity (Pa·s)
v	Kinematic viscosity (m^2/s)
ρ	Density (kg/m^3)

Subscripts:

tot	Total, both oil and water
o	Oil
tt	Turbulent-turbulent
w	Water

ACKNOWLEDGEMENTS

The authors gratefully acknowledge the financial support of OneSubsea, funding from the Department of Mechanical and Nuclear Engineering to fund G.A.R., and the assistance of Jarrod Booth in collecting the data.

References

[1] Bannwart, A. C., 2001, "Modeling aspects of oil–water core–annular flows," Journal of Petroleum Science and Engineering, 32(2), pp. 127-143.

[2] Cai, J., Li, C., Tang, X., Ayello, F., Richter, S., and Nesic, S., 2012, "Experimental study of water wetting in oil–water two phase flow—Horizontal flow of model oil," Chemical Engineering Science, 73, pp. 334-344.

[3] Bultongez, K. K., and Derby, M. M., 2017, "Investigation of oil-water flow regimes and pressure drops in mini-channels," International Journal of Multiphase Flow, 96, pp. 101-112.

[4] Andreini, P., De Greeff, P., Galbiati, L., Kuhlwetter, A., and Sotgia, G., "Oil-water flow in small diameter tubes," Proc. ICHMT DIGITAL LIBRARY ONLINE, Begel House Inc.

[5] Kandlikar, S. G., and Grande, W. J., "Evolution of microchannel flow passages: thermohydraulic performance and fabrication technology," Proc. ASME 2002 International Mechanical Engineering Congress and Exposition, American Society of Mechanical Engineers, pp. 59-72.

[6] Brauner, N., and Moalem Maron, D., "'Classification of Liquid-Liquid Two-Phase Flow Systems and The Prediction of Flow Pattern Maps," Proc. 2nd International Symposium on Two-Phase Flow Modeling and Experimentation–ISTP, pp. 747-754.

[7] Taitel, Y., and Dukler, A., 1976, "A model for predicting flow regime transitions in horizontal and near horizontal gas-liquid flow," AIChE Journal, 22(1), pp. 47-55.

[8] Xu, J. L., Cheng, P., and Zhao, T. S., 1999, "Gas-liquid two-phase flow regimes in rectangular channels with mini/micro gaps," International Journal of Multiphase Flow, 25, pp. 411-432.

343 [9] Garimella, S., 2004, "Condensation Flow Mechanisms in Microchannels: Basis for Pressure
344 Drop and Heat Transfer Models," Heat Transfer Engineering, 25(3), pp. 104-116.
345 [10] Coleman, J. W., and Garimella, S., 2003, "Two-phase flow regimes in round, square and
346 rectangular tubes during condensation of refrigerant R134a," International Journal of
347 Refrigeration, 26(117-128).
348 [11] Kandlikar, S. G., 2002, "Two-phase flow patterns, pressure drop, and heat transfer during
349 boiling in minichannel flow passages of compact evaporators," Heat Transfer Engineering,
350 23(1), pp. 5-23.
351 [12] Revellin, R., and Thome, J., 2007, "A new type of diabatic flow pattern map for boiling heat
352 transfer in microchannels," Journal of Micromechanics and Microengineering, 17(4), p. 788.
353 [13] Brauner, N., and Ullmann, A., 2002, "Modeling of phase inversion phenomenon in two-
354 phase pipe flows," International Journal of Multiphase Flow, 28(7), pp. 1177-1204.
355 [14] Beretta, A., Ferrari, P., Galbiati, L., and Andreini, P., 1997, "Horizontal oil-water flow in
356 small diameter tubes. Flow patterns," International communications in heat and mass transfer,
357 24(2), pp. 223-229.
358 [15] Bultongez, K. K., and Derby, M. M., "Oil-water flow visualization and flow regimes in a
359 3.7 mm mini-channel," Proc. Proceedings of the 14th International Conference on Nanochannels,
360 Microchannels, and Minichannels (ICNMM).
361 [16] Grassi, B., Strazza, D., and Poesio, P., 2008, "Experimental validation of theoretical models
362 in two-phase high-viscosity ratio liquid–liquid flows in horizontal and slightly inclined pipes,"
363 International Journal of Multiphase Flow, 34(10), pp. 950-965.

[17] Sotgia, G., Tartarini, P., and Stalio, E., 2008, "Experimental analysis of flow regimes and pressure drop reduction in oil–water mixtures," International Journal of Multiphase Flow, 34(12), pp. 1161-1174.

[18] Lovick, J., and Angeli, P., 2004, "Experimental studies on the dual continuous flow pattern in oil–water flows," International Journal of Multiphase Flow, 30(2), pp. 139-157.

[19] da Silva, R. C. R., Mohamed, R. S., and Bannwart, A. C., 2006, "Wettability alteration of internal surfaces of pipelines for use in the transportation of heavy oil via core-flow," Journal of Petroleum Science and Engineering, 51(1), pp. 17-25.

[20] Arney, M. S., Ribeiro, G. S., Guevara, E., Bai, R., and Joseph, D. D., 1996, "Cement-lined pipes for water lubricated transport of heavy oil," International Journal of Multiphase Flow, 22(2), pp. 207-221.

[21] Ismail, A. S. I., Ismail, I., Zoveidavianpoor, M., Mohsin, R., Piroozian, A., Misnan, M. S., and Sariman, M. Z., 2015, "Experimental investigation of oil–water two-phase flow in horizontal pipes: Pressure losses, liquid holdup and flow patterns," Journal of Petroleum Science and Engineering, 127, pp. 409-420.

[22] Wang, W., Gong, J., and Angeli, P., 2011, "Investigation on heavy crude-water two phase flow and related flow characteristics," International Journal of Multiphase Flow, 37(9), pp. 1156-1164.

[23] Xu, X.-X., 2007, "Study on oil–water two-phase flow in horizontal pipelines," Journal of Petroleum Science and Engineering, 59(1), pp. 43-58.

[24] Li, C., Tang, X., Ayello, F., Cai, J., Nesic, S., Cruz, C. I. T., and Al-Khamis, J. N., 2006, "Experimental study on water wetting and CO2 corrosion in oil-water two-phase flow," NACE Corrosion, 6.

[25] Oglesby, K. D., 1979, An experimental study on the effects of oil viscosity, mixture velocity and water fraction on horizontal oil-water flow, University of Tulsa, Fluid Flow Projects.

[26] Tsaoulidis, D., Dore, V., Angeli, P., Plechkova, N. V., and Seddon, K. R., 2013, "Flow patterns and pressure drop of ionic liquid–water two-phase flows in microchannels," International Journal of Multiphase Flow, 54, pp. 1-10.

[27] Brauner, N., 2003, "Liquid-liquid two-phase flow systems," Modelling and Experimentation in Two-Phase Flow, Springer, pp. 221-279.

[28] Salim, A., Fourar, M., Pironon, J., and Sausse, J., 2008, "Oil–water two-phase flow in microchannels: Flow patterns and pressure drop measurements," The Canadian Journal of Chemical Engineering, 86(6), pp. 978-988.

[29] Foroughi, H., and Kawaji, M., 2011, "Viscous oil–water flows in a microchannel initially saturated with oil: flow patterns and pressure drop characteristics," International Journal of Multiphase Flow, 37(9), pp. 1147-1155.

[30] Yun, W., Ross, C. M., Roman, S., and Kovscek, A. R., 2017, "Creation of a dual-porosity and dual-depth micromodel for the study of multiphase flow in complex porous media," Lab on a Chip, 17(8), pp. 1462-1474.

[31] Xu, K., Liang, T., Zhu, P., Qi, P., Lu, J., Huh, C., and Balhoff, M., 2017, "A 2.5-D glass micromodel for investigation of multi-phase flow in porous media," Lab on a Chip, 17(4), pp. 640-646.

[32] Schmitz, E. A., 2018, "Impacts of industrial water composition on Salicornia in a hydroponic system," M.S., Kansas State University, Manhattan, KS.

[33] Rulison, C., 2018, "Augustine Report April 11 2018," Augustine Scientific.

[34] Brauner, 2004, "Liquid-Liquid two-phase flow systems," CISM Center, Udine, Italy.

[35] De, B., Mandal, T., and Das, G., 2010, "The rivulet flow pattern during oil–water horizontal flow through a 12 mm pipe," Experimental Thermal and Fluid Science, 34(5), pp. 625-632.

[36] Jovanović, J., Zhou, W., Rebrov, E. V., Nijhuis, T., Hessel, V., and Schouten, J. C., 2011, "Liquid–liquid slug flow: hydrodynamics and pressure drop," Chemical Engineering Science, 66(1), pp. 42-54.

[37] Charles, M. E., Govier, G. t., and Hodgson, G., 1961, "The horizontal pipeline flow of equal density oil-water mixtures," the Canadian Journal of Chemical engineering, 39(1), pp. 27-36.

[38] Kim, S.-M., and Mudawar, I., 2013, "Universal approach to predicting saturated flow boiling heat transfer in mini/micro-channels–Part II. Two-phase heat transfer coefficient," International Journal of Heat and Mass Transfer, 64, pp. 1239-1256.

[39] Kim, S.-M., and Mudawar, I., 2012, "Flow condensation in parallel micro-channels–Part 2: Heat transfer results and correlation technique," International Journal of Heat and Mass Transfer, 55(4), pp. 984-994.